doi:10.11835/j.issn.1671-8224.2017.02.01

To cite this article: ZHANG Peng, WANG Meng, BAO Bing-bing. Non-undercutting condition and parameter optimization for cycloid ball planetary transmission [J]. J Chongqing Univ Eng Ed [ISSN 1671-8224], 2017, 16(2):51-58.

Non-undercutting condition and parameter optimization for cycloid ball planetary transmission *

ZHANG Peng †, WANG Meng, BAO Bing-bing

School of Mechanical Engineering, Anhui University of Technology, Maanshan, Anhui Province 243032, P. R. China,

Received 18 October 2016; received in revised form 7 March 2016

Abstract: The transmission performance of cycloid ball planetary transmission (CBPT) is affected by cycloid tooth undercutting directly, and the design of CBPT can be optimized by the non-undercutting condition. Firstly, the theoretical equation of cycloid tooth is given, and the curvature radius of cycloid tooth profile is derived. Secondly, according to the relationship between the curvature radius and the distribution circle of balls, the non-undercutting condition of cycloid tooth profile is established, and the non-undercutting critical condition is deduced. Finally, the validity of the non-undercutting critical condition is verified by simulation. The result shows that the non-undercutting critical condition can be used to optimize the design of CBPT.

Keywords: cycloid ball; planetary transmission; tooth profile; non-undercutting condition; parameter optimization

CLC number: TH132 Document code: A

1 Introduction

The undercutting of cycloid tooth is a difficulty of the cycloid ball planetary transmission (CBPT), which has great influence on cycloid tooth design and tooth shape optimization. Furthermore, the synthesis curvature of engagement pair and the pressure angle of cycloid tooth profile are changed by the undercutting of cycloid tooth, and the transmission ability and reliability are decreased [1]. Although many scholars have done theoretical research on the cycloid ball planetary transmission including reliability optimization [2-3], dynamics analysis [4-5], and value selection of cycloid curtate ratio [6-7], the research of non-undercutting design method is reported rarely, and the judgment method of the non-undercutting condition is never given. This paper focuses on the problem of cycloid undercutting. According to the relationship between the cycloid curvature radius and ball radius, the minimum function of the undercutting condition is obtained, and the design criteria of cycloid with non-undercutting can be acquired using this function.

2 The structure and working principle

Fig. 1 shows the structure of CBPT. The epicycloid groove is milled on the left side of planetary disc, of

† ZHANG Peng (张鹏): pengzhang1980@aliyun.com.

* Funded by the National Natural Science Foundation of China (Grant No.51405003).

which tooth number is Z_1. The hypocycloid groove is milled on the right side of central disc, of which tooth number is Z_2. The CBPT is a two-tooth differenced planetary transmission [8], so the relationship of teeth is $Z_2 - Z_1 = 2$. The balls are installed in the stagger zone of the epicycloid groove and hypocycloid groove, whose number is Z_0, and $Z_0 = (Z_1 + Z_2)/2$. The epicycloid groove, hypocycloid groove, and balls form the cycloid ball engagement pair.

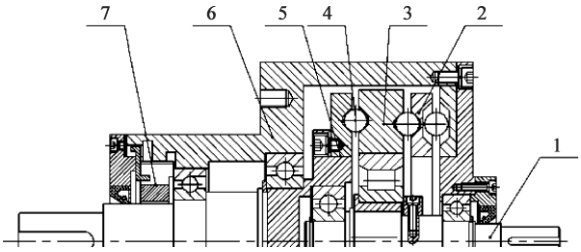

Legend:

1. Eccentric input shaft; 2. Equal velocity mechanism;

3. Planetary disc; 4. Ball; 5. Central disc; 6. Casing;

7. Clearance adjustment screw.

Fig. 1 The structure of cycloid ball planetary transmission

The eccentric input shaft drives the planetary disc to move, the planetary disc is restricted by the equal velocity mechanism, and then moves with translational motion. At the same time, the epicycloid groove on planetary disc pushes the balls to move, and the central disc is pushed by the balls to rotate slowly. The velocity variation is completed.

3 Theoretical tooth profile equation and curvature radius

The theoretical tooth profile equation of trochoidal cycloid and the curvature radius are given to solve the non-undercutting condition of cycloid tooth. In this paper, the curvature radius of cycloid tooth with a convex is defined as positive. The curvature radius of cycloid tooth with a concave is defined as negative.

3.1 Theoretical tooth profile equation and curvature radius of epicycloid

Epicycloid is the path of a point within the occurrence circle, which rolls on the base circle. The theoretical tooth profile equation of epicycloid is expressed as follows.

$$\begin{cases} x_1 = R_0 \cos\theta_1 - Kr_0 \cos\left[\left(1+Z_1\right)\theta_1\right], \\ y_1 = R_0 \cos\theta_1 - Kr_0 \sin\left[\left(1+Z_1\right)\theta_1\right], \end{cases} \tag{1}$$

where x_1 and y_1 are the coordinates of epicycloid; R_0 is the radius of the ball distribution circle; r_0 is the radius of the occurrence circle; K is the cycloid curtate ratio; and θ_1 is the epicycloid generation angle.

According to the curvature formula of plane curve [9], the theoretical tooth profile curvature radius of epicycloid can be expressed as

$$\rho_1 = \frac{R_0\sqrt{\left[1+K^2-2K\cos\left(Z_1\theta_1\right)\right]^3}}{1+K_2Z_0-KZ_2\cos\left(Z_1\theta_1\right)}, \tag{2}$$

where $\rho_1$is the theoretical tooth profile curvature radius of epicycloid.

The parameters of cycloid tooth are shown in Table 1. According to Formula (2) and Table 1, the theoretical tooth profile curvature radius of epicycloid with one tooth is obtained as shown in Fig. 2.

Table 1 The parameters of cycloid tooth

Parameter	Z_1	Z_2	Z_0	R_0/mm	K
Value	29	31	30	90	0.2

In Fig. 2, the period of epicycloid generation angle with one tooth is from 0° to 360°. When the epicycloid generation angle is from 0° to 60°, the theoretical tooth profile of epicycloid is a concave, and the curvature radius increases. When the epicycloid generation angle is about 60°, the tooth profile is changed from a

concave to a convex; When the epicycloid generation angle is from 60° to 310°, the theoretical tooth profile curvature radius of epicycloid decreases firstly then increases; When the angle is about 310°, the tooth profile is changed to a concave again, and then the curvature radius decreases.

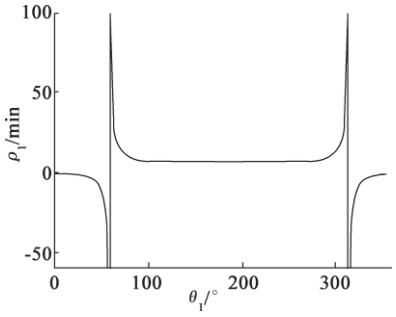

Fig. 2 Theoretical tooth profile curvature radius of epicycloid ρ_1 changing with the epicycloid generation angle θ_1

3.2 Theoretical tooth profile equation and curvature radius of hypocycloid

A hypocycloid is the path of a point within the occurrence circle, which rolls in the base circle. The theoretical tooth profile equation of hypocycloid is expressed as follows.

$$\begin{cases} x_2 = R_0 \cos\theta_2 + Kr_0 \cos\left[\left(1-Z_2\right)\theta_2\right], \\ y_2 = R_0 \cos\theta_2 + Kr_0 \sin\left[\left(1-Z_2\right)\theta_2\right], \end{cases} \tag{3}$$

where x_2 and y_2 are the coordinates of the hypocycloid; θ_2 is the hypocycloid generation angle.

According to the curvature formula of plane curve [9], the theoretical tooth profile curvature radius of hypocycloid can be expressed as

$$\rho_2 = \frac{R_0\sqrt{\left[1+K^2-2K\cos\left(Z_2\theta_2\right)\right]^3}}{1-K^2Z_0+KZ_1\cos\left(Z_2\theta_2\right)}, \tag{4}$$

where ρ_2 is the theoretical tooth profile curvature radius of hypocycloid.

According to Formula (3) and Table 1, the theoretical tooth profile curvature radius of hypocycloid with one tooth is obtained as shown in Fig. 3.

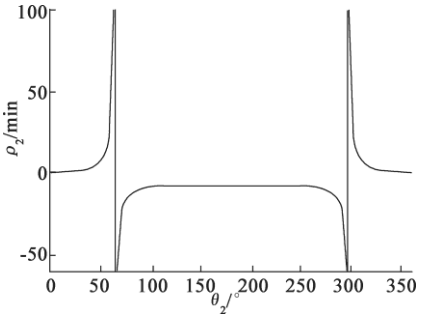

Fig. 3 Theoretical tooth profile curvature radius of hypocycloid ρ_2 changing with the hypocycloid generation angle θ_2

In Fig. 3, the period of hypocycloid generation angle with one tooth is from 0° to 360°. When the hypocycloid generation angle is from 0° to 60°, the theoretical tooth profile of hypocycloid is a convex, and the curvature radius increases. When the hypocycloid generation angle is about 60°, the tooth profile is changed from a convex to a concave. When the hypocycloid generation angle is from 60° to 310°, the curvature radius increases firstly then decreases. When the hypocycloid generation angle is about 300°, the tooth profile is changed to a convex again, and then the curvature radius decreases.

4 Establishment of non-undercutting condition

The transmission effect is affected negatively by the undercutting of cycloid tooth, so the judgment method of undercutting condition is very important. Whether the undercutting of cycloid tooth happens or not can be judged by the relationship between the cycloid curvature radius and the ball radius, so the non-undercutting condition of cycloid tooth can be

established by this relationship.

4.1 Non-undercutting condition of epicycloid tooth

Fig. 4 shows the engagement pair of a cycloid groove and a ball. In Fig. 4, r is the radius of ball; β is the angle of cycloid groove, which is 45° generally. The undercutting will make the cusp of cycloid tooth, then cause the contact stress increasing and part life decreasing.

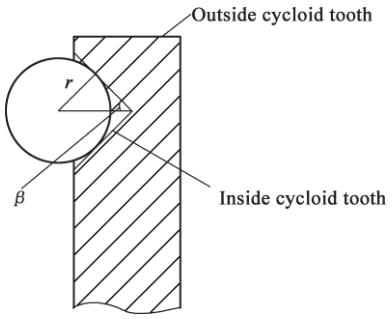

Fig. 4 The engagement pair of cycloid groove and ball, where r is the radius of ball; and β is the angle of cycloid groove

4.1.1 Non-undercutting condition of epicycloid outside tooth

According to the curvature radius of epicycloid outside tooth, the non-undercutting conditions of epicycloid outside tooth is as follows.

A. When the tooth profile is convex, $\rho_1 > 0$, $\rho_1 + r\cos\beta > 0$ is always satisfied, and the undercutting of epicycloid outside tooth never happens.

B. When the tooth profile is concave, $\rho_1 < 0$, and $\rho_1 < -r\cos\beta$ must be satisfied.

Combining conditions A and B, the non-undercutting condition of epicycloid outside tooth is:

$$\rho_1 + r\cos\beta < 0. \tag{5}$$

According to Formulas (2) and (5), the non-undercutting condition of epicycloid outside tooth can be simplified as:

$$\left(-\frac{S^{\frac{3}{2}}}{T}\right)_{\min} > \frac{r\cos\beta}{R_0}, \tag{6}$$

where $S = \sqrt{\left[1 + K^2 - 2K\cos\left(Z_1\theta_1\right)\right]^3}$; and $T = 1 + K_2 Z_0 - KZ_2\cos\left(Z_1\theta_1\right)$.

4.1.2 Non-undercutting condition of epicycloid inside tooth

According to the curvature radius of epicycloid inside tooth, and the non-undercutting condition of epicycloid inside tooth is as follows.

C. When the tooth profile is convex, $\rho_1 > 0$, and $\rho_1 - r\cos\beta > 0$ must be satisfied.

D. When the tooth profile is concave, $\rho_1 < 0$, $\rho_1 - r\cos\beta < 0$ is always satisfied, and the undercutting of epicycloid inside tooth never happens.

Combining conditions C and D, the non-undercutting condition of epicycloid inside tooth is:

$$\rho_1 > r\cos\beta. \tag{7}$$

According to Formulas (2) and (7), the non-undercutting condition of epicycloid outside tooth can be simplified as

$$\left(\frac{S^{\frac{3}{2}}}{T}\right)_{\min} > \frac{r\cos\beta}{R_0}. \tag{8}$$

4.1.3 Non- undercutting condition of epicycloid

According to Formulas (6) and (8), the non-undercutting condition of epicycloid can be obtained as

$$\begin{cases}\left(-\dfrac{S^{\frac{3}{2}}}{T}\right)_{\min} > \dfrac{r\cos\beta}{R_0}, \dfrac{S^{\frac{3}{2}}}{T} < 0; \\ \left(\dfrac{S^{\frac{3}{2}}}{T}\right)_{\min} > \dfrac{r\cos\beta}{R_0}, \dfrac{S^{\frac{3}{2}}}{T} > 0. \end{cases} \tag{9}$$

4.2 Non-undercutting condition of hypocycloid tooth

4.2.1 Non-undercutting condition of hypocycloid outside tooth

According to the curvature radius of hypocycloid outside tooth, the non-undercutting condition of hypocycloid outside tooth is as follows.

E. When the tooth profile is convex, $\rho_2 > 0$, $\rho_2 + r\cos\beta > 0$ is always satisfied, and the undercutting of hypocycloid outside tooth never happens.

F. When the tooth profile is concave, $\rho_2 < 0$, and $\rho_2 < -r\cos\beta$ must be satisfied.

Combining condition E and condition F, the non-undercutting condition of hypocycloid outside tooth is:

$$\rho_2 < -r\cos\beta. \tag{10}$$

According to Formulas (4) and (10), the non-undercutting condition of hypocycloid outside tooth can be simplified as:

$$\left(-\frac{S^{\frac{3}{2}}}{U}\right)_{\min} > \frac{r\cos\beta}{R_0}, \tag{11}$$

where $U = 1 - K^2 Z_0 + KZ_2\cos(Z_2\theta_2)$.

4.2.2 Non-undercutting condition of hypocycloid inside tooth

According to the curvature radius of hypocycloid inside tooth, the non-undercutting condition of hypocycloid inside tooth is as follows.

G. When the tooth profile is convex, $\rho_2 > 0$, and $\rho_2 > r\cos\beta$ must be satisfied.

H. When the tooth profile is concave, $\rho_2 < 0$, $\rho_2 - r\cos\beta < 0$ is always satisfied, and the undercutting of hypocycloid inside tooth never happens.

Combining Conditions G and H, the non-undercutting condition of hypocycloid inside tooth is

$$\rho_2 > r\cos\beta. \tag{12}$$

According to Formulas (4) and (12), the non-undercutting condition of hypocycloid inside tooth can be simplified as

$$\left(\frac{S^{\frac{3}{2}}}{U}\right)_{\min} > \frac{r\cos\beta}{R_0}. \tag{13}$$

4.2.3 Non-undercutting condition of hypocycloid

According to Formulas (11) and (13), the non-undercutting condition of hypocycloid can be obtained as

$$\begin{cases}\left(-\dfrac{S^{\frac{3}{2}}}{U}\right)_{\min} > \dfrac{r\cos\beta}{R_0}, \dfrac{S^{\frac{3}{2}}}{U} < 0; \\ \left(\dfrac{S^{\frac{3}{2}}}{U}\right)_{\min} > \dfrac{r\cos\beta}{R_0}, \dfrac{S^{\frac{3}{2}}}{U} > 0. \end{cases} \tag{14}$$

4.3 Non-undercutting condition of the CBPT

According to Sections 4.1 and 4.2, the non-undercutting condition of the CBPT can be obtained as

$$\frac{r\cos\beta}{R_0} < \left[\left(-\frac{S^{\frac{3}{2}}}{T}\right)_{\min}, \left(\frac{S^{\frac{3}{2}}}{T}\right)_{\min}, \left(-\frac{S^{\frac{3}{2}}}{U}\right)_{\min}, \left(\frac{S^{\frac{3}{2}}}{U}\right)_{\min}\right]_{\min}. \tag{15}$$

5 Non-undercutting critical condition

5.1 Solution of non-undercutting condition for epicycloid tooth

In order to solve the non-undercutting condition of epicycloid tooth, Formula (9) is transformed as follows.

$$\frac{S^{\frac{3}{2}}}{T}=\frac{\sqrt{\left[1+K^2-2K\cos\left(Z_1\theta_1\right)\right]^3}}{1+K_2Z_0-KZ_2\cos\left(Z_1\theta_1\right)}. \tag{16}$$

Let $\theta_b=Z_1\theta_1$, the extreme value points of Formula (16) can be solved as follows.

$$\theta_b=\begin{cases}0^\circ \text{ when } \dfrac{1}{Z_0}<K<1;\\ 180^\circ \text{ when } K\le\dfrac{Z_0-2}{2Z_0-1};\\ \arccos\dfrac{3-Z_2+\left(3Z_0-Z_2\right)K_2}{Z_2K}\\ \qquad \text{when } \dfrac{Z_0-2}{2Z_0-1}<K<1;\\ 2\pi-\arccos\dfrac{3-Z_2+\left(3Z_0-Z_2\right)K_2}{Z_2K}\\ \qquad \text{when } \dfrac{Z_0-2}{2Z_0-1}<K<1.\end{cases} \tag{17}$$

Formula (17) expresses the possible places of extreme value points. Taking these points into Formula (16), the non-undercutting condition of epicycloid in the extreme value points is obtained as follows.

When $\theta_b=0^\circ$,

$$\left(-\frac{S^{\frac{3}{2}}}{T}\right)_{\min}=\frac{-\left(1-K\right)^3}{1+K^2Z_0-KZ_0}. \tag{18}$$

When $\theta_b=180^\circ$,

$$\left(\frac{S^{\frac{3}{2}}}{T}\right)_{\min}=\frac{\left(1+K\right)^3}{1+K^2Z_0+Z_2K}. \tag{19}$$

When

$$\theta_b=\begin{cases}\arccos\dfrac{3-Z_2+\left(3Z_0-Z_2\right)K_2}{Z_2K}\\ 2\pi-\arccos\dfrac{3-Z_2+\left(3Z_0-Z_2\right)K_2}{Z_2K}\end{cases},$$

$$\left(\frac{S^{\frac{3}{2}}}{T}\right)_{\min}=\frac{\left(3+3K^2-\dfrac{6\left(1+Z_0K^2\right)}{Z_2}\right)^{\frac{3}{2}}}{-2-2Z_0K^2+\left(1+K^2\right)Z_2}. \tag{20}$$

5.2 Solution of non-undercutting condition for hypocycloid tooth

The non-undercutting condition of hypocycloid tooth can be obtained by solving the extreme value points of Formula (14), and the method is same as in Section 5.1. The non-undercutting condition of hypocycloid in the extreme value points is obtained as follows.

When $\theta_b=0^\circ$,

$$\left(\frac{S^{\frac{3}{2}}}{U}\right)_{\min}=\frac{\left(1-K\right)^3}{1-K^2Z_0+Z_1K}. \tag{21}$$

When $\theta_b=180^\circ$,

$$\left(-\frac{S^{\frac{3}{2}}}{U}\right)_{\min}=\frac{-\left(1+K\right)^3}{1-K^2Z_0-Z_1K} \tag{22}$$

When

$$\theta_b=\begin{cases}\arccos\dfrac{\left(2Z_1+3\right)K^2-3-Z_1}{Z_1K},\\ 2\pi-\arccos\dfrac{\left(2Z_1+3\right)K^2-3-Z_1}{Z_1K},\end{cases}$$

$$\left(-\frac{S^{\frac{3}{2}}}{U}\right)_{\min}=\frac{-\left(3+3K^2-\frac{6\left(Z_0K^2-1\right)}{Z_1}\right)^{\frac{3}{2}}}{-2-Z_1+\left(2Z_0-Z_1\right)K^2}. \tag{23}$$

5.3 Non-undercutting critical condition of CBPT

Compare the calculated results of Formulas (18) to (23), and take them into Formula (15). The non-undercutting critical condition of CBPT can be obtained as follows:

$$\frac{r\cos\beta}{R_0}<\frac{\left(1-K\right)^3}{1-K^2Z_0+Z_1K}. \tag{24}$$

The undercutting happens on the hypocycloid inside tooth first in CBPT [10], and Formula (24) is the non-undercutting critical condition for the hypocycloid inside tooth actually. The cycloid groove with non-undercutting tooth can be designed and optimized by Formula (24).

6 Simulation and manufacture

The parameters of CBPT prototype are shown in Table 2. According to Formula (24), the cycloid parameters with non-undercutting condition are given as: K=0.2, and R_0=90 mm.

Table 2 Parameters of CBPT prototype

Parameter	Z_1	Z_2	Z_0	r/mm
Value	29	31	30	10

According to the parameters of Table 2, the tooth profile equations of epicycloid and hypocycloid are calculated, and the 3D models are generated using software Pro-E in Figs. 5 and 6.

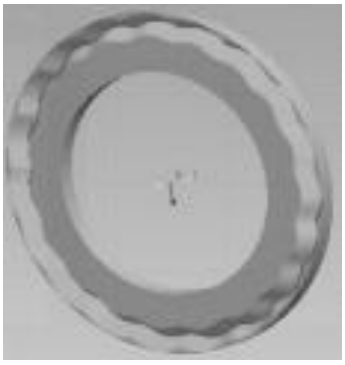

Fig. 5 The 3D model of epicycloid tooth

Fig. 6 The 3D model of hypocycloid tooth

Fig. 7 is the simulation of cycloid tooth using the software Mastercam_X5, and the interference phenomenon caused by undercutting never happens in simulation.

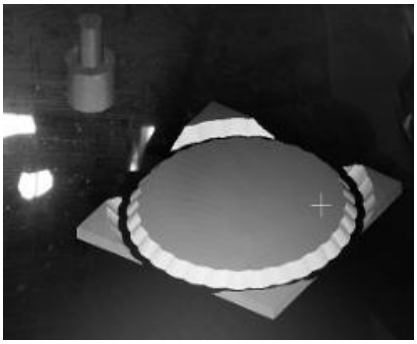

Fig. 7 The simulation with Mastercam_X5

Fig. 8 shows the manufacture of cycloid disc.

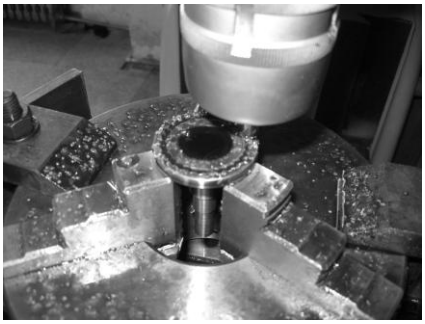

Fig. 8 The manufacture of cycloid tooth

7 Conclusion

1) The non-undercutting condition of cycloid tooth profile for CBPT is researched. The non-undercutting critical condition of cycloid tooth profile is solved by the analysis of cycloid tooth profile and curvature radius, and the result is verified by simulation.

2) The critical position of undercutting changes with the variation of tooth profile parameters. The undercutting happens on the hypocycloid inside tooth first in CBPT.

3) The CBPT with undercutting can be designed by the non-undercutting condition, and the design process can be simplified by the non-undercutting critical condition of hypocycloid inside tooth especially.

References

[1] 叶仲和,张炜,黄清海,等.摆线转子泵小转子不根切的条件[J].机械设计与研究,2004,20(5):36-38.
YE Z H, ZHANG W, HUANG Q H, et al. Cycloid rotor pump rotor is not small cutting conditions [J]. Journal of Mechanical Design and Research, 2004, 20(5): 36-38. (In Chinese).

[2] 安子军,王广欣.摆线钢球行星传动的模糊可靠性优化设计[J].机械传动,2004,28(5):17-20.
AN Z J, WANG G X. The fuzzy reliability optimum design of cycloid steel ball planetary transmission [J]. Journal of Mechanical Transmission, 2004, 28(5): 17-20. (In Chinese).

[3] 张鹏,安子军,杨作梅.摆线钢球行星传动啮合副非线性力学性能研究[J].工程力学,2010,27(3):186-192.
ZHANG P, AN Z J, YANG Z M. Research on nonlinear mechanical properties for engagement pair of cycloid ball planetary transmission [J]. Journal of Engineering Mechanics, 2010, 27(3): 186-192. (In Chinese).

[4] 张鹏,安子军.摆线钢球行星传动动力学建模与固有特性分析[J].中国机械工程,2014,25(2):157-161.
ZHANG P, AN Z J. Dynamics model and natural characteristics of cycloid ball planetary transmission [J]. China Mechanical Engineering, 2014, 25(2): 157-161. (In Chinese).

[5] 安子军,张鹏,杨作梅.摆线钢球行星传动系统参数振动特性研究[J].工程力学,2012, 29(3):244-251.
AN Z J, ZHANG P, YANG Z M. Research on properties for parametric vibration of cycloid ball planetary transmission system [J]. Engineering Mechanics, 2012, 29(3): 244-251. (In Chinese).

[6] 王文涛,徐宏海,刘学翱,等.短幅摆线及其齿廓特性的理论研究[J].机械设计与制造,2016,(1):94-97.
WANG W T, XU H H, LIU X A, et al. The theoretical study about characteristics of curtate cycloid and its tooth profile [J]. Journal of Mechanical Design and Manufacturing, 2016, (1) : 94-97. (In Chinese).

[7] 蔡峰,张鹏,张玉华,等.摆线钢球行星传动中短幅系数取值方法研究[J].机械传动,2014,38(3):27-30.
CAI F, ZHANG P, ZHANG Y H, et al. Study on value select method of curtate ratio of cycloid ball planetary transmission [J]. Journal of Mechanical Transmission, 2014, 20(3): 27-30. (In Chinese).

[8] TERADA H, IMASE K. Fundamental analysis of a cycloid ball reducer (5th Report) - development of a two stage type reduction mechanism [J]. JSPE, 2009, 75(12): 1418-1422.

[9] RUI J G. Numerical simulation of liner curvature radius on formation of LEFP [J]. Advanced Materials Research, 2014, 3226(941): 2305-2308.

[10] 杨作梅,安子军,张鹏.基于空间啮合理论的摆线钢球行星传动根切研究[J].农业机械学报,2009,40(10):216-222.
YANG Z M, AN Z J, ZHANG P. Research on undercutting in cycloid ball planetary transmission based on space meshing theory [J]. Journal of Agricultural Machinery, 2009, 40(10): 216-222. (In Chinese).